Modification of Tryptophan and Methionine Residues Is Implicated in the Oxidative Inactivation of Surfactant Protein B

Dahis Manzanares,[‡,§] Karina Rodriguez-Capote,[‡] Suya Liu,[||] Thomas Haines,[‡] Yudith Ramos,[||] Lin Zhao,[‡] Amanda Doherty-Kirby,[||] Gilles Lajoie,[||] and Fred Possmayer*[,‡,||]

Department of Obstetrics and Gynaecology and Department of Biochemistry, Schulich School of Medicine and Dentistry, The University of Western Ontario, London, ON, Canada N6A 5C1

Received November 7, 2006; Revised Manuscript Received February 13, 2007

ABSTRACT: Exposing BLES (bovine lipid extract surfactant), a clinical surfactant, to reactive oxygen species (ROS) alters surfactant protein B (SP-B), as indicated by Coomassie Blue staining, silver staining, and Western analysis. Hypochlorous acid (HOCl) treatment leads to elevated maximum surface tension (γ_{max}) and a deterioration in minimum γ (γ_{min}) during surface area cycling. Fenton reaction resulted in immediate increases in γ_{min} and γ_{max}. Intrinsic fluorescence measurements indicated Fenton, but not HOCl, induced conversion of Trp9 of SP-B to hydroxyTrp (OHTrp), *N*-formylkynurenine (NFKyn), and kynurenine (Kyn). Electrospray ionization mass spectrometry (ESI-MS) revealed molecular weight alterations consistent with oxidation of Met (HOCl, Fenton) and Trp (Fenton) residues. Oxidative alterations to Met29 and Met65 (HOCl, Fenton) and to Trp9 (OHTrp with HOCL and NFKyn plus Kyn with Fenton) were confirmed by matrix-assisted laser desorption mass spectrometry (MALDI-MS) studies on SP-B tryptic fragments. Some Met oxidation was observed with control SP-B. When taken together with captive bubble tensiometer measurements, these studies suggest that Met oxidation of SP-B by HOCl or Fenton interferes with phospholipid respreading during compression−expansion of surfactant films, while Fenton oxidation, which produces more extensive Met oxidation and disruption of the indole ring of Trp9, further abrogated the ability of such films to attain low surface tensions during compression. These studies provide insight into the manner by which ROS generated during acute lung injury and the acute respiratory distress syndrome act to inhibit not only endogenous surfactant but also therapeutic surfactants administered to counteract these conditions.

Pulmonary surfactant is essential for normal lung function. Surfactant reduces the work of breathing during inflation and stabilizes the alveoli during expiration (*1*−*4*). In addition, surfactant contributes to mucociliary transport and functions as an inflammatory-reducing factor in pulmonary host defense (*5*, *6*). Surfactant is composed of lipids (mainly phospholipids (PL[1])) and the surfactant-associated proteins SP-A, SP-B, SP-C, and SP-D (*7*). SP-A and SP-D are water-soluble, collagen-containing lectins (collectins) which function in host defense, while SP-B and SP-C are low molecular weight, hydrophobic proteins which coextract with surfactant lipids. SP-B and SP-C contribute to the surface-active properties of pulmonary surfactant and are crucial components of the modified natural surfactants used to treat surfactant deficiency associated with the neonatal respiratory distress syndrome (RDS). SP-B deficiency leads to death from respiratory distress (*3*, *4*, *8*, *9*).

In addition to its well-established role in RDS, considerable evidence has accumulated which demonstrates that pulmonary surfactant function can become impaired during induction of acute lung injury (ALI) and the acute respiratory distress syndrome (ARDS) (*2*, *10*−*13*). Although ALI and ARDS arise from a variety of insults, primary and secondary increases in ROS are a common factor in the pathophysiology of these conditions (*12*, *14*−*16*). Although early studies largely focused on interactions of ROS with surfactant PLs, it has become evident that the deleterious effects of ROS also impact on surfactant proteins (*17*−*23*). For example, our laboratory has conducted reconstitutive experiments, employing surfactant lipids and hydrophobic proteins isolated from control and oxidized pulmonary surfactant, using the captive bubble tensiometer (CBT) (*23*). The CBT is an artificial alveolus model which can be used to follow adsorption of surfactant PL to form a surface-active film. In addition, this apparatus can be used to follow surface tension during quasi-static or dynamic surface area compression−

* Corresponding author. Phone: (519) 661-2111 x80972. Fax: (519) 661-3175. E-mail: fpossmay@uwo.ca.

‡ Department of Obstetrics and Gynaecology.

§ Present address: Division of Pulmonary and Critical Care Medicine, Department of Medicine, Miller School of Medicine, University of Miami, Miami, FL.

|| Department of Biochemistry.

[1] Abbreviations: γ, surface tension; ALI, acute lung injury; ARDS, acute respiratory distress syndrome; BLES, bovine lipid extract surfactant; BSA, bovine serum albumin; CBT, captive bubble tensiometer; C∼, H∼, and F∼SP-B, SP-B isolated from control, HOCl-treated, or Fenton-treated BLES; DPPC, dipalmitoylphosphatidylcholine; ESI-MS, electrospray ionization mass spectrometry; HOCl, hypochlorous acid; Kyn, kynurenine; MALDI-MS, matrix-assisted laser desorption mass spectrometry; NFKyn, *N*-formyl kynurenine; OHTrp, hydroxytryptophan; PL, phospholipid; POPG, 1-palmitoyl-2-oleoyl-*sn*-phosphatidylglycerol; RDS, respiratory distress syndrome; ROS, reactive oxygen species; SDS−PAGE, sodium dodecylsulfate−polyacrylamide gel; SP-, surfactant protein.

10.1021/bi062304p CCC: $37.00
Published on Web 04/11/2007

expansion cycles, mimicking processes occurring in the lung in vivo. These reconstitution studies demonstrated that ROS reduced surface activity by affecting surfactant PL, SP-B, and SP-C, but the most dramatic effect was due to ROS-induced inactivation of SP-B (*23*).

These and similar findings (*12*, *19*) prompted further investigations to obtain insight into the manner by which ROS reacts with SP-B, a dimer of two identical polypeptides of 79 amino acids structurally related to the saposin family, to which also belongs NK-lysin (*24*). Monomeric SP-B is thought to contain four or five amphipathic alpha helices (*9*, *25*, *26*). The SP-B dimers are thought stabilized by an intersubunit disulfide bridge, Cys48−Cys48′, and by the interactions between Glu51 to Arg52′ and Glu51′ with Arg52 (*27*). In the lung, in vivo, SP-B likely associates directly with the surface tension (γ)-reducing surface monolayer (*28*, *29*) and thus will be exposed to oxidants present in the environment (e.g., air pollutants, cigarette smoke) (*30*), as well as those generated in the alveolar hypophase (e.g., during inflammation) (*12*, *14*, *15*, *17*). As indicated earlier, previous studies have provided evidence indicating that ROS modifications to SP-B are a major contributor to surfactant inactivation (*12*, *19*, *23*, *31*). However, the nature of the modifications to SP-B induced during oxidative stress has not been determined.

The present studies investigate the effects of hypochlorous acid and Fenton reaction products on SP-B structure and function. These investigations show that the major effects of HOCl are to oxidize Met, while the Fenton reaction affects both Trp and Met. While both HOCl and Fenton oxidation hamper surfactant biophysical activity, under the conditions used the more potent effects are observed with Fenton reaction.

MATERIALS AND METHODS

Materials. All reagents were purchased from Sigma/Aldrich (St. Louis, MO) and/or VWR/Canlab (Mississauga, ON) unless otherwise noted. BLES was a kind gift of BLES Biochemicals, Inc., London, ON. Dipalmitoylphosphatidylcholine (DPPC) was purchased from Sigma/Aldrich, and 1-palmitoyl, 2-oleoyl, phosphatidylglycerol-sodium salt (POPG) was obtained from Avanti Polar Lipids (Birmingham, AL).

Hypochlorous acid was purchased as sodium hypochlorite (NaOCl) from Sigma/Aldrich specified with an active chlorine content of 10−13%. The hypochlorite concentration was determined spectrophotometrically immediately before use by diluting the NaOCl stock solution 1:10 in 1 M NaOH at 240 nm using a molar extinction coefficient for pH 12 of 43.6 mol^{-1} cm^{-1}.

In Vitro Oxidation. BLES. Reaction mixtures were composed of 10 mg/mL surfactant lipids, plus Fenton reagents, hypochlorous acid or control BLES in working buffer (in mM): 0.150 NaCl, 20 Tris-HCl, and 1.5 $CaCl_2$ at pH 7.4. The samples were incubated at 37 °C in a shaking water bath, normally for 24 h. For standard oxidation by the Fenton-like chemistry, BLES at 10 mg/mL was incubated with 0.65 mM $FeCl_2$, 0.65 mM sodium ethylenediamine tetraacetic acid (EDTA), and 30 mM H_2O_2 in working buffer at a pH of 7.4 (*17*, *23*, *31*). Treatment with HOCl/$^-$OCl was carried out at a final concentration of 0.5 mM at pH 7.4 in working buffer. After oxidation or control incubations, the lipid fraction was isolated by the method of Bligh and Dyer (*32*) and conserved at −20 °C until the various components were fractionated.

Isolation of SP-B. Pulmonary SP-B was isolated from control or oxidized BLES by a modification of the LH-60 method of Curstedt et al. (*33*) as previously described (*34*, *35*). Absorbance at 260 and 280 nm was used to monitor protein isolation during chromatography.

Protein concentrations were determined by a modification of the method of Lowry et al. (*34*, *36*). Correction factors of 2.0 for SP-B and 3.0 for SP-C relative to bovine serum albumin (BSA) were adopted on the basis of amino acid analysis as indicated previously (*31*, *37*). The purity of the proteins was routinely assessed by sodium dodecylsulfate (SDS)−polyacrylamide gel (PAGE) using 18% gels (*38*), and for residual PL contamination by phosphorus determination.

Protection Assays. For the protection studies, we carried out oxidation of SP-B in the presence and absence of lipids, normally using 200 μg/mL of isolated SP-B with and without 800 μg of DPPC:POPG (7:3). The same standard conditions were used for hypochlorous (0.5 mM NaOCl) and Fenton (0.65 mM Fe^{2+}/EDTA; 30 mM H_2O_2) oxidation; control peptide was exposed to the same conditions without the oxidants (37 °C, with stirring). After 4 h or 24 h of incubation, samples were taken for analysis and biophysical activity.

Electrophoresis and Western Blot Analysis. For SP-B analysis, nonreduced samples were separated on SDS−PAGE and stained with Coomassie Blue or silver reagent (Invitrogen, Burlington, ON), as indicated. In some cases, 4−20% Novex gradient gels (Invitrogen) were used. For Western blot analysis, samples were subsequently electroblotted onto hydrophobic polyvinylidene difluoride (PVDF) membranes Immobilon-P^{SQ} (Millipore Inc., Dedford, MA). These membranes were blocked in 5% nonfat dry milk dissolved in TTBS (150 mM NaCl, 10 mM Tris-HCl, 0.1% Tween 20, pH 7.4) and incubated thereafter for 1 h at room temperature with a monoclonal antibody against SP-B (kindly donated by Dr. Y. Suzuki, Kyoto University, Japan) (*39*), followed by washing and incubation for 1 h with horseradish peroxidase-conjugated rabbit anti-mouse immunoglobulin. A chemoluminiscent kit (Supersignal West Fempto, BioLynx Inc., Brockville, ON) was used to develop the reaction. Immunoreactive bands were visualized by using Kodak Biomax XAR film. This antiserum recognizes bovine, human, rabbit, and rat SP-B by Western blotting and does not cross-react with SP-A, SP-C, rat serum proteins, or BSA.

Captive Bubble Tensiometry. CBT assays were normally performed in triplicate, using 400 μg/mL of PL in working buffer. Adsorption, quasi-static, and dynamic experiments were conducted as described previously (*31*, *35*). Briefly, after the CBT chamber was filled with a suspension of the desired surfactant, an air bubble, 5−8 mm diameter, is introduced. Changes in bubble shape were recorded to monitor the adsorption of the surface-active materials to the air−saline interface. When equilibrium surface tension (γ_{eq}) was achieved, the chamber was sealed and quasi-static or dynamic compression−expansion cycles were performed. Changes in bubble area were recorded during each individual experiment and the bubble shapes analyzed using custom

designed software to calculate the surface tension of the film (*31*, *35*, *40*). For dynamic cycling, once the film adsorbed to γ_{eq}, one quasi-static compression−expansion cycle was conducted to establish surface area reduction required to attain minimum surface tension (γ_{min}). The γ_{min} was established either as the lowest γ attainable without bubble clicking (defined as an abrupt change to a small surface area with a higher γ) or γ near 1.0 mN/m. Dynamic modes were then implemented by cycling the bubble between 100% and 110% of the original surface area and the area required to achieve γ_{min} at 30 cycles per minute.

For the evaluation of the activity of reconstituted surfactants, control or oxidized SP-Bs at a concentration of 1% SP-B with respect to DPPC:POPG (7:3) (400 μg/mL) were suspended in 2 mL of CBT buffer. Adsorption, quasi-static and dynamic cycling were assayed in the CBT as above.

Fluorescence Spectroscopic Studies. Fluorescence measurements were normally carried out on a Fluorolog-3 spectrofluorometer (Horiba Jobin Yvon, Edison, NJ). For measuring fluorescence of isolated SP-B proteins in methanol, cells of 1 cm optical path were used and slits were kept at 5 nm. In a typical experiment, 50 μg/mL of SP-B in methanol was excited at 275, 325, 360, or 450 nm and the emission spectra were recorded as indicated. At least ten scans were analyzed for each sample.

Electrospray Ionization Mass Spectrometry (ESI-MS) Analysis. ESI-MS was carried on a Q-TOF (Micromass, Manchester, U.K.) instrument. For the recording of positive ion mass spectra, 10 μL samples, in $CHCl_3/CH_3OH$ (1:1 v/v), were loaded into a gold coated glass capillary (Proxeon Biosystems, Odense, Denmark). The capillary orifice was opened 5 to 10 μm. The electrospray voltage, cone voltage, and collision energy were set to approximately 1600, 50, and 10 V, respectively. The instrument was tuned to resolution of 8000 or more and calibrated using NaI over a range of 400 to 4000 *m*/*z*. A mass accuracy of 50 ppm was routinely obtained as estimated from the results of analysis of a standard solution of myoglobin. Deconvolution of the ESI data was done using maximum entropy software (Masslynx 4.0).

Matrix-Assisted Laser Desorption Ionization Mass Spectrometry (MALDI-MS). Coomassie Blue-stained SP-B bands were cut out of the SDS−PAGE gels and in-gel-digested using established methods (*41*). Briefly, the gel bands were washed, destained, reduced with Tris(2-carboxyethyl)phosphine hydrochloride (TCEP) (Sigma/Aldrich, Oakville, ON, Canada), alkylated with iodoacetamide (Sigma/Aldrich), and then digested with 0.2 μg of trypsin (Promega, Madison, WI) in 50 μL of $(NH_4)_2CO_3$ (100 mM, pH 7.8) at 37 °C for 24 h. The tryptic peptides were extracted from the gel bands with 50% acetonitrile and 5% formic acid. The α-cyano-4-hydroxycinnamic acid (Sigma/Aldrich) matrix was prepared at 10 mg/mL in acetonitrile/ethanol/trifluoroacetic acid (0.1%) (49.5/49.5/1, v/v/v). Tryptic digested SP-B sample, 1 μL, was mixed with 1 μL of matrix solution and spotted onto a target plate prior to being loaded into the mass spectrometer for analysis.

MALDI mass spectra were recorded on a Micromass MALDI−R mass spectrometer (Micromass, Manchester, U.K.) equipped with a nitrogen pulsed laser (337 nm) operating in positive-ion-reflector mode. The pulse voltage, the source voltage and the reflectron voltage were set at 3000, 15 000, and 500 V, respectively. Spectra were collected in a range of *m*/*z* 900 and 4000. The instrument was tuned to a resolution of 10 000 and externally calibrated using a mixture of peptides. The overall mass accuracy was better than 0.05 Da for the *m*/*z* range used.

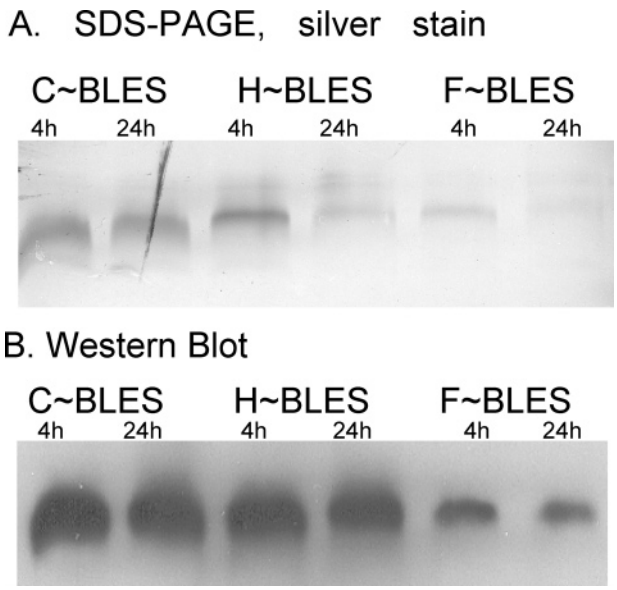

FIGURE 1: Effect of exposing BLES to hypochlorous acid or Fenton reagents on SP-B chemical and immunochemical reactivity. BLES was treated at 37 °C for 4 or 24 h, and samples were taken immediately for electrophoresis, silver staining, and Western blotting for SP-B. From left to right: C∼BLES 4 h, C∼BLES 24 h, H∼BLES 4 h, H∼BLES 24 h, F∼BLES 4 h, F∼BLES 24 h.

Statistical Analysis. Standard error of the means was obtained from samples of $n = 3$ or greater. Statistical comparisons were conducted using SPSS (Chicago, IL) software. Comparisons between the three groups were conducted by analysis of variance (ANOVA) followed by Bonferroni and Tukey post-hoc tests. Post-hoc analysis refers to the statistical analysis between individual groups only if the ANOVA shows a significant difference between the groups as a whole. Probability values below 0.05 are considered significant.

RESULTS

Effects of ROS on SP-B Reactivity and Biophysical Activity. Previous studies have indicated that exposing pulmonary surfactant to ROS results in structural alterations in surfactant apoproteins as well as surfactant lipids. Treating BLES with pathophysiological levels of hypochlorous acid (H∼BLES) for 4 or 24 h at 37 °C resulted in a decrease in silver staining and a slight depression in Western blot immunoreactivity using a specific anti-SP-B antibody relative to control (C∼BLES) (Figure 1). Exposure to Fenton reagents (F∼BLES) for 4 or 24 h resulted in markedly reduced detectability with either procedure (Figure 1). In contrast, 24 h treatment under these conditions had no significant effect on organic solvent-extractable lipid phosphorus levels (*42*) (H∼BLES, 100.2 ± 1.1%; F∼BLES, 102.4 ± 1.8%, relative to C∼BLES, $n = 3$) or in protein levels (H∼BLES, 94.5 ± 3.4%, F∼BLES, 121.5 ± 14.5% of C∼BLES, $n = 6$), measured using a modification (*34*) of the method of Lowry et al. (*36*). The observation that ROS treatment does not impact seriously on estimates of BLES

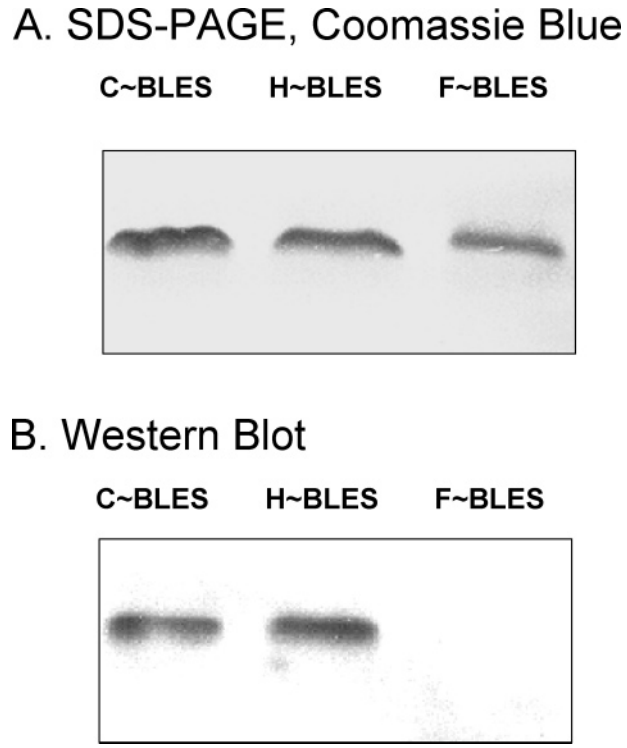

FIGURE 2: Electrophoretic analyses of SP-B isolated from control and oxidized BLES. SP-B fractions obtained by LH-60 chromatography were analyzed after PAGE electrophoresis. (A) 4 μg of proteins were loaded and stained with Coomassie Blue. (B) SP-B detected by Western blot analyses. With the actual gels, SP-B from H-BLES shows a slight decline in Western staining while SP-B from F-BLES can barely be detected.

surfactant apoproteins is important in that it allows direct comparisons of Lowry based equivalents on SDS−PAGE gels. When identical amounts (by Lowry) of SP-B, isolated from C∼BLES (C∼SP-B), H∼BLES (H∼SP-B), or F∼BLES (F∼SP-B) were analyzed by electrophoresis, F∼SP-B and, to a lesser extent, H∼SP-B displayed depressed staining to Coomassie Blue on SDS−PAGE gels (Figure 2A). Furthermore, Western blot analyses revealed that H∼SP-B activity showed slightly depressed reactivity relative to C∼SP-B (Figure 2B), while F∼SP-B could barely be detected. Taken together, these results indicate that the decreased immunodetection of F∼SP-B in Figures 1 and 2 is not the result of changes induced by the isolation procedure but is caused by the oxidation itself. The results also show that the oxidative effects are progressive.

Reconstitution studies employing as PL, DPPC:POPG (7:3), and 1% SP-B isolated from C∼BLES, H∼BLES, and F∼BLES revealed slower adsorption to equilibrium for H∼SP-B:DPPC:POPG (10.9 ± 1.3 min) and F∼SP-B:DPPC:POPG (14.5 ± 1.3 min) relative to C∼SP-B:DPPC:POPG (2.0 ± 0.2 min) (Figure 3A). Results obtained during dynamic surface area cycling experiments revealed that C∼SP-B:DPPC:POPG and H∼SP-B:DPPC:POPG were capable of attaining γ_{min}s less than 5 mN/m during initial dynamic compression, but F∼SP-B:DPPC:POPG reconstitutes could not lower γ below 10 mN/m (Figure 3B). Furthermore, with prolonged surface area cycling, C∼SP-B:DPPC:POPG maintained its surface activity, but the surface activity of H∼SP-B:DPPC:POPG deteriorated such that by the 21st dynamic cycle, γ_{min} for the reconstitute was similar to that for F∼SP-B:DPPC:POPG during either the first or

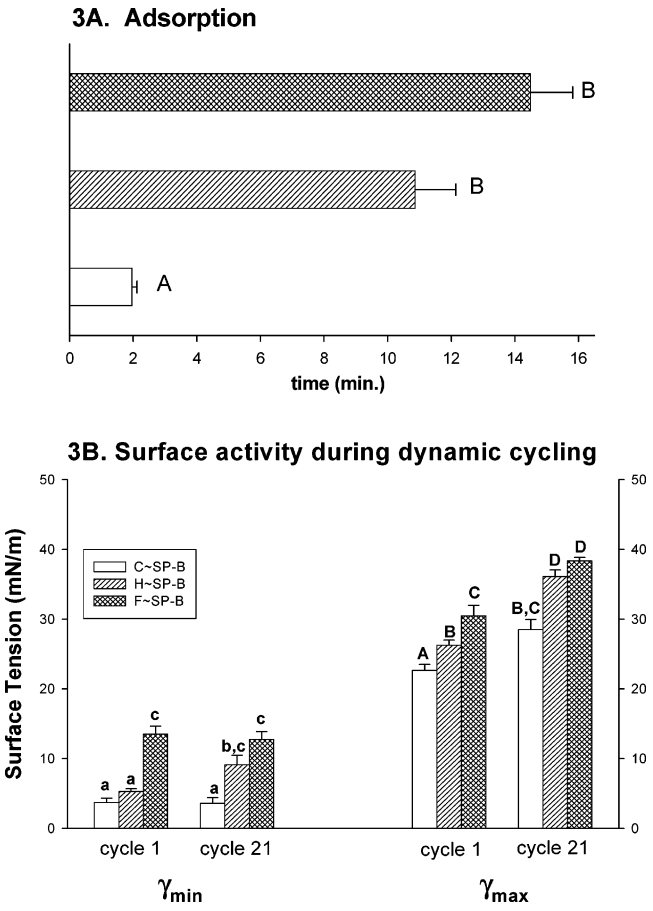

FIGURE 3: Biophysical activity of SP-B isolated from control, hypochlorous acid-treated, and Fenton-treated BLES. Isolated SP-Bs were reconstituted as DPPC:POPG:SP-B (70:30:1), and dispersions (400 μg in saline:1.5 mM $CaCl_2$) were examined with a captive bubble surfactometer. (A) Adsorption isotherms for SP-B from control, hypochlorous acid-treated (H), and Fenton reaction-exposed (F) BLES. SP-Bs from oxidized BLES exhibited greatly impaired film formation. (B) Minimum and maximum surface tensions for reconstituted surfactants during the initial and 21st dynamic cycle. Letters represent comparisons for adsorption or within the cycle depicted. Means with the same letter are not significantly different.

21st dynamic cycle (Figure 3B). The maximum γ values also increased with oxidized SP-Bs. Similar overall results were observed using PL recovered from control BLES for reconstitution (not shown). These observations are consistent with ROS-induced alterations to certain amino acids in SP-B which are involved in reactivity with Coomassie Blue and in anti-SP-B Ab recognition. The results are also consistent with ROS-induced alterations in SP-B which interfere with the ability of this low molecular weight, hydrophobic protein to increase the adsorption of surfactant PL and to promote γ reduction to low values during surface area reduction.

Effect of ROS on BLES Tryptophan. For these studies, SP-B and SP-C were isolated from control and oxidized BLES by monitoring absorbance at 260 and 280 nm during chromatography on LH-60. With C∼BLES, the 260/280 nm ratio for the C∼SP-B peak was ∼0.85, while that for C∼SP-C was ∼1.2, consistent with the exclusive presence of Trp and Tyr in SP-B. Interestingly, fractions isolated from H∼BLES displayed 260/280 nm ratios of ∼ 0.9, while F∼SP-B showed values of ∼1.2, indicating that Fenton and possibly hypochlorous oxidation affected the characteristic

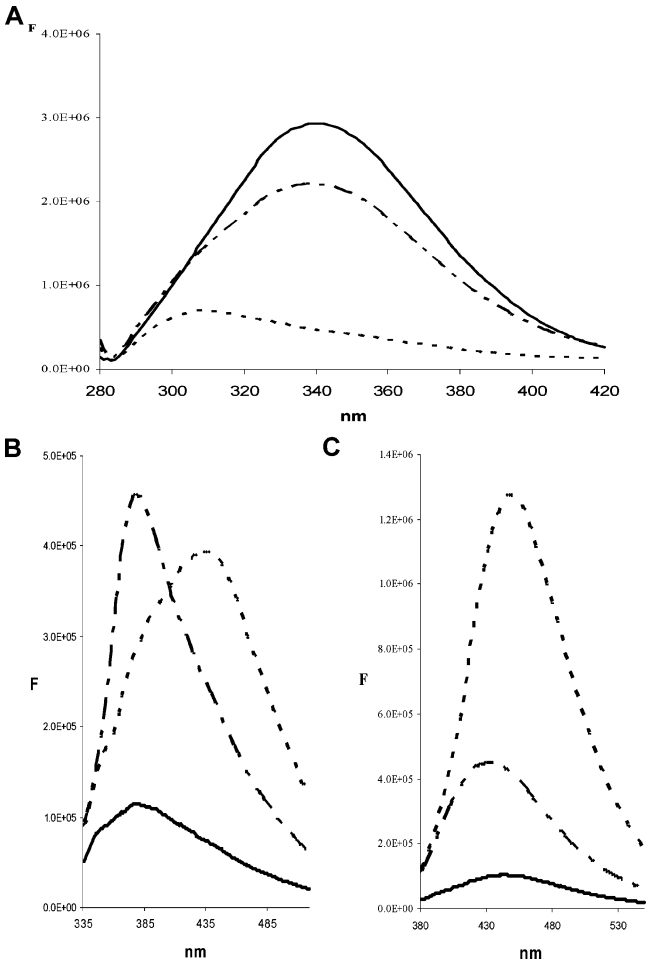

FIGURE 4: Fluorescence emission spectra for C∼SP-B, H∼SP-B, and F∼SP-B. Emission spectra of isolated SP-Bs (50 μg/mL) in methanol. C∼SP-B (solid line); H∼SP-B (dashed line); F∼SP-B (dotted line). (A) Emission spectrum at $\lambda_{exc} = 275$ nm showing that the intrinsic fluorescence associated with aromatic residues is strongly decreased for F∼SP-B. (B) For $\lambda_{exc} = 325$, a peak at 435 nm suggests the presence of NFKyn in F∼SP-B; a nonidentified peak is observed for H∼SP-B. (C) The presence of Kyn is indicated in F∼SP-B at $\lambda_{exc} = 365$ nm and $\lambda_{em} = 449$ nm.

absorbance due to aromatic amino acids. Since it has been reported that aromatic amino acids are targets for oxidative alterations in soluble proteins, we employed fluorescence spectroscopy to investigate modifications to SP-B.

Representative emission spectra at $\lambda_{Eex} = 275$ nm reveal that C∼SP-B possesses a maximum emission at 340 nm, corresponding to the typical fluorescence attributed to aromatic residues Trp and Tyr present in the protein (Figure 4A). A similar, albeit decreased, intensity spectrum was observed for H∼SP-B. The spectrum obtained for F∼SP-B indicated that aromatic amino acids were greatly affected by Fenton oxidation. Control experiments using excitation at 295 nm to avoid spectral effects of Tyr modification gave similar results (data not shown).

The inference that Fenton oxidation induced chemical modifications in the Trp residue of SP-B was reinforced by fluorescence detection of specific products reported to occur in other oxidized proteins (*43*−*45*). Examination of F∼SP-B spectra produced evidence for Trp oxidation to *N*-formylkynurenine (NFKyn) ($E_{Ex} = 325$ nm, $E_{Em} = 425$ nm) (Figure 4B) and kynurenine (Kyn) ($E_{Ex} = 365$ nm, $E_{Em} = 449$ nm) (Figure 4C). Evidence was also obtained for the possible cross-linking of Kyn (not shown). The fluorescence emission scanning experiments suggested only slight Trp modification during hypochlorous acid-induced oxidation of BLES, when compared with C∼BLES. Excitation at 325 nm generated an unidentified emission peak at 379 nm. In addition, enhanced emissions were always observed compared to C∼SP-B when the protein was excited at 365 or 450 nm. These results are in agreement with the weaker fluorescence emissions for Trp at 275 nm (Figure 4A).

ROS Effects on BLES SP-B as Detected by ESI-MS. Figure 5A depicts positive ESI-MS spectra for SP-B isolated from control and oxidized BLES. The recorded spectra showed predominant peaks in *m*/*z* range from 1000 to 2200 corresponding to 5 to 13 charged SP-B ions (Figure 5A, upper panel). Deconvolution of the spectrum for control SP-B (Figure 5B, top panel) shows a protein peak with molecular mass of 17397.4 Da. This mass perfectly matches the calculated mass of SP-B, 17397.4 Da, using the sequence presented in Table 1. It is also consistent with the presence of an SP-B dimer as suggested by SDS−PAGE electrophoresis (Figures 1, 2B). The deconvoluted spectrum also revealed a minor peak with an increase in mass of ∼15 Da (17 412.6 Da), probably reflecting the average mass increases due to a single oxidation (16 Da) and methylation (14 Da) of SP-B. This indicates that C∼SP-B is partially oxidized and methylated, likely during incubation at 37 °C, isolation on LH-60 with chloroform:methanol:HCl and/or analyses.

The ESI-MS spectra of SP-B isolated from H∼BLES revealed a similar overall pattern to C∼BLES, but the overall peak distribution was altered. Deconvolution of this spectrum gave the most intense protein peak a molecular mass of 17 460.3 Da, 63 Da heavier than actual SP-B, corresponding to a SP-B dimer with four oxidized Met (Figure 5B, middle panel). It also revealed a greater number of readily identifiable peaks with incremental mass increases of ∼16 Da, indicating occurrence of oxidation of other amino acids. Different preparations of H∼BLES showed slightly different patterns for oxidized SP-B (data not shown), suggesting some heterogeneity in the reaction.

The ESI-MS spectra for F∼SP-B displayed a much higher background ionization with only three major peaks accompanied by very wide peaks indicating that aggregation may have occurred. Deconvolution of the spectrum showed a great number of peaks with incremental mass increases of 14 to 16 Da. The most intense protein peak showed a mass of 17468.2 Da. The exact structural modifications of SP-B could not be determined from this mass increase alone, but this mass increase is consistent with dimeric SP-B containing four oxidized Met and two NFKyn.

MALDI-MS Analyses of SP-B. In order to obtain further information with respect to modifications introduced into BLES during oxidation by hypochlorous acid and the Fenton reaction, SP-Bs were separated on SDS−PAGE and the bands cut out, reduced, treated with iodoacetamide to prevent sulfhydryl reoxidation, and digested with trypsin. The trypsin fragments were then extracted and analyzed by MALDI-MS.

Table 1 presents the amino acid sequence for mature bovine SP-B recently obtained by tandem MS analysis of tryptic digested SP-B and cDNA sequencing (Liu, S. et al., to be submitted elsewhere). According to this amino acid sequence, it can be predicted that SP-B will generate eight peptides among which four peptides will have suitable

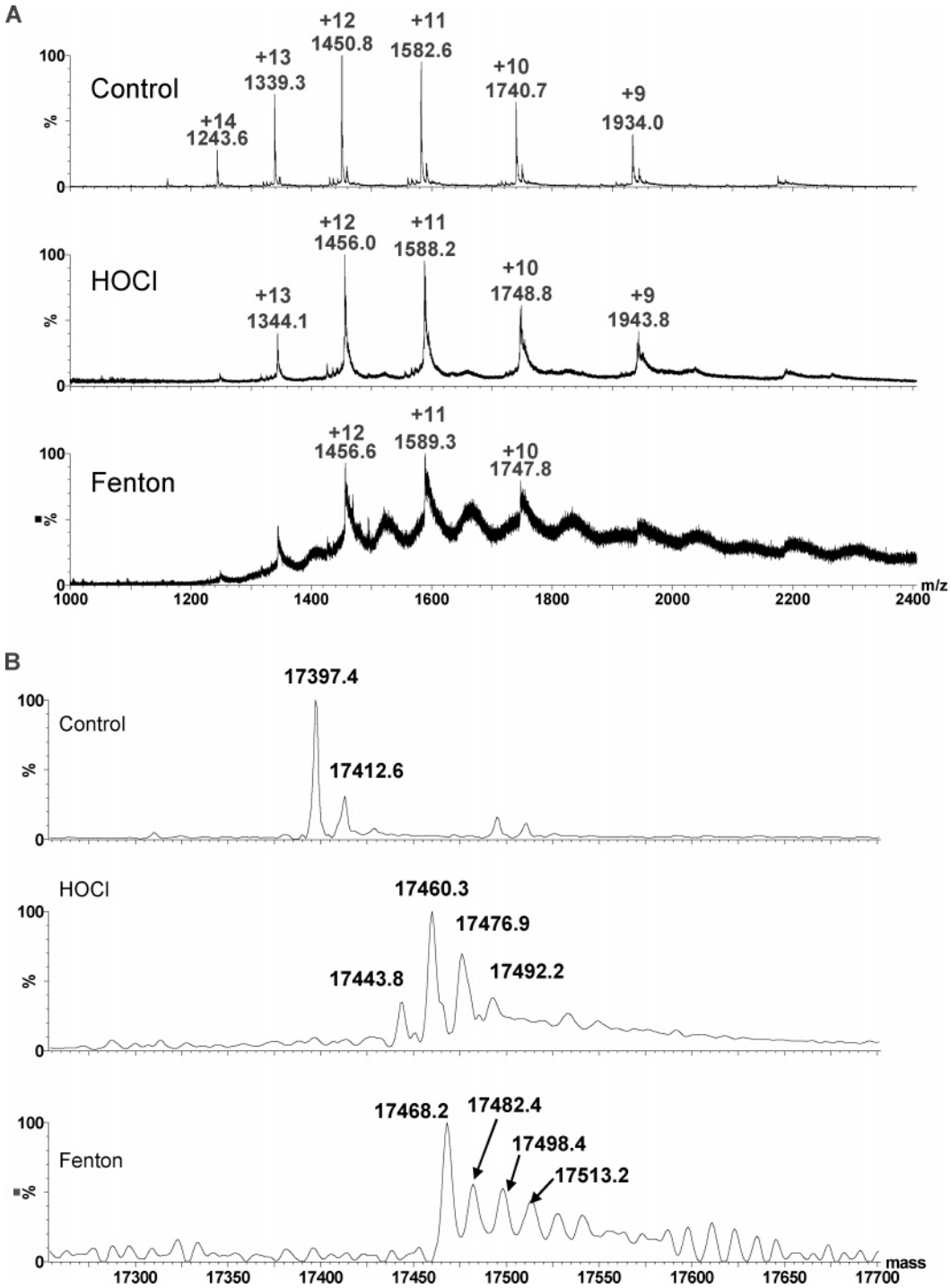

FIGURE 5: ESI-MS spectra of isolated oxidized SP-Bs (A) and their deconvoluted spectra (B), as described in the text.

Table 1: Amino Acid Sequences for Bovine SP-B and for Four Predicted Tryptic Peptides (T1,5,6,7) Generated by the ExPasy Proteomic Tools[a]

average mass = 9105.2

1	6	11	16	21	26	31	36	41	46	51	56	61	66	71	76
FPIPI	PYCWL	CRTLI	KRIQA	VIPKG	VLAMT	VAQVC	HVVPL	LVGGI	CQCLV	ERYSV	ILLDT	LLGRM	LPQLV	CGLVL	RCSS

fragment	residues	sequence	[M + H]
T1	1−12	(−) FPIPIPYCWLCR (T)	1621.8
T5	25−52	(K) GVLAMTVAQVCHVVPLLVGGI CQCLV ER	3078.6
T6	53−64	(R) YSVILLDTLLGR (M)	1362.8
T7	65−76	(R) MLPQLVCGLVLR (C)	1398.8

masses for MALDI-MS (*m*/*z* 1000−4000). Figure 6A, B, and C show mass spectra for *m*/*z* 1330−1450, 1600−1700, and 2960−3220, respectively. The major peak at 1362.8 *m*/*z* in Figure 6A corresponds to T6 (Y53−R64) (numbering

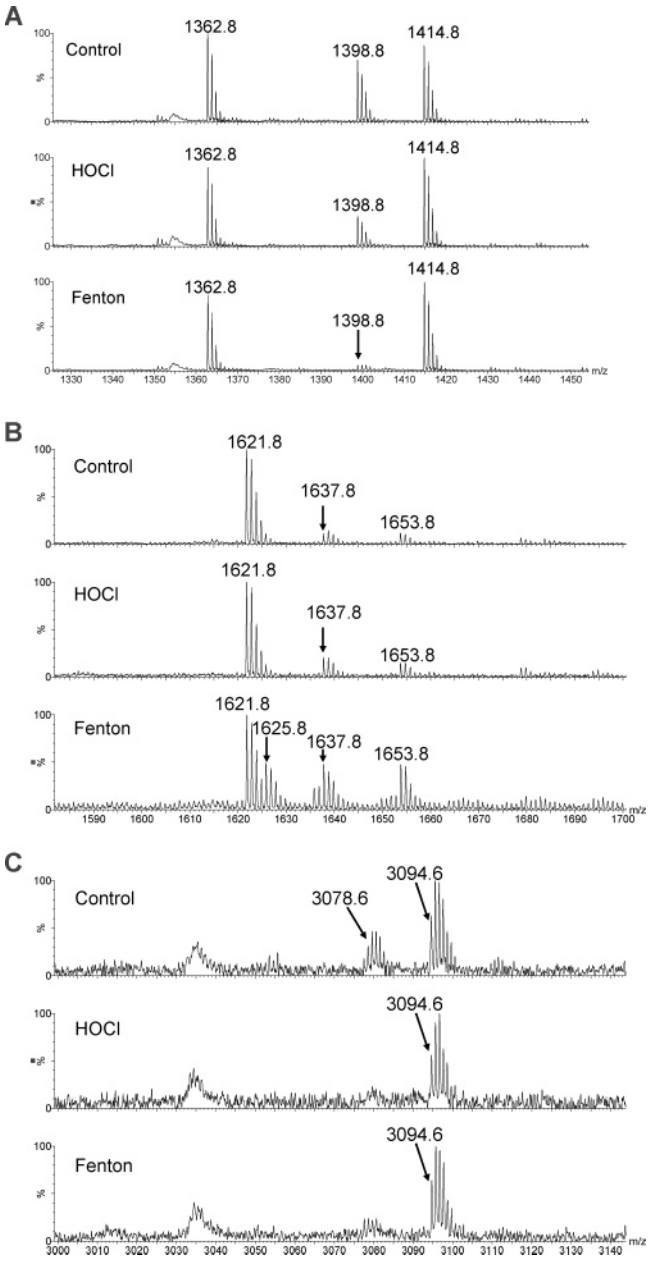

FIGURE 6: MALDI spectra of tryptic peptides from C∼SP-B, H∼SP-B, and F∼SP-B, as described in the text. Peptide sequences for C∼SP-B in A, B, and C are as listed in Table 1.

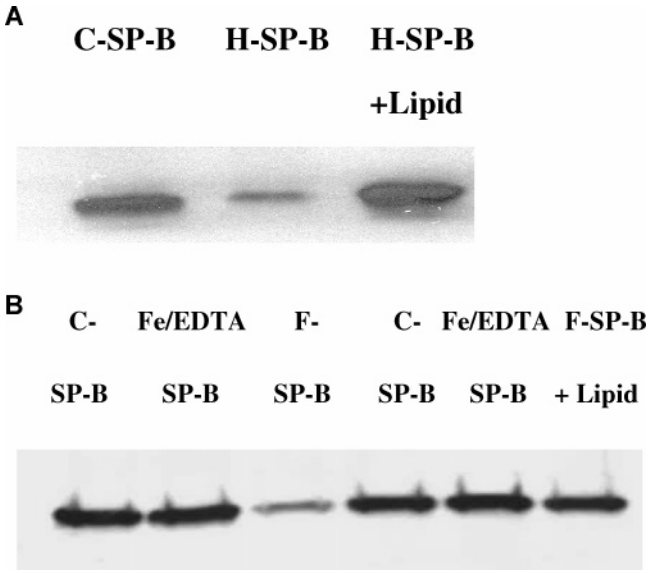

FIGURE 7: Effect of lipids on the resistance of native SP-B to hypochlorous acid or Fenton oxidation. SP-Bs were treated as indicated below, separated by SDS−PAGE and detected by Western blot analysis. (A) Isolated SP-B obtained from C∼BLES was treated for 2 h at 37 °C. From left to right: control SP-B (no lipids), hypochlorous oxidized SP-B (no lipids), hypochlorous oxidized SP-B previously reconstituted with DPPC:POPG (7:3). (B) Isolated SP-B from C∼BLES was incubated at 37 °C for 24 h. From left to right: control SP-B (no lipids), Fe/EDTA-treated SP-B (no lipids), Fenton-oxidized SP-B (no lipids), control SP-B, Fe/EDTA-treated SP-B, and Fenton-oxidized SP-B previously reconstituted with DPPC:POPG (7:3).

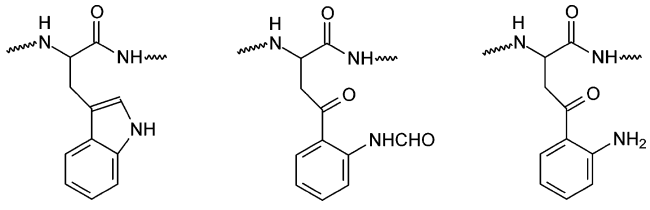

FIGURE 8: Molecular structures for Trp, NFKyn, and Kyn.

according to the theoretical digestion pattern). No oxidation products were observed with noticeable intensity for this peptide in any of four samples.

The peak at 1398.8 *m*/*z* corresponds to peptide T7 (M65−R76), while the peak at 1414.8 *m*/*z* corresponds to oxidized T7. Considerable oxidation of T7, as manifested by the 1398.8/1414.8 ratio, was observed even with control incubated BLES. Nevertheless, the oxidized T7 peak was increased slightly in spectra of H∼SP-B and greatly with F∼SP-B samples, indicating occurrence of Met65 oxidation upon H and F treatment. The 1398.8 peak is slightly diminished with H∼SP-B and almost obliterated with F∼SP-B, accompanied by corresponding increases in the 1414.8 peak.

In Figure 6B, the peak at 1621.8 corresponds to peptide T1 (F1−R12). Minor peaks observed at 1637.8 and 1653.8 in the control spectrum (Figure 5B, first panel) indicate single and double additions of oxygen, most likely due to oxidation of Trp9 (see Discussion). These results also indicate that C∼SP-B is partially oxidized. The 1637.8 *m*/*z* peak is most likely attributable to the formation of hydroxytryptophan (OHTrp), while the 1653.8 *m*/*z* peak could be dihydroxytryptophan (DiOHTrp) or NFKyn. These peaks were slightly elevated in H∼SP-B and markedly increased in F∼SP-B spectra compared to C∼SP-B. In addition, a peak at 1625.8 is clearly elevated with F∼SP-B. This peak could correspond to a peptide containing Kyn (structure shown in Figure 8) formed by the loss of the *N*-formyl group from the Trp indole ring during oxidation (*46*, *47*). Separate experiments employing tandem MS confirmed the presence of OHTrp, DiOHTrp (or NFKyn), and Kyn in the appropriate F∼SP-B peaks (data not shown). In addition to the above, a minor peak at 1635.8 *m*/*z* was observed in the spectrum of F∼SP-B (Figure 6B, third panel), which shows a 14 Da increase over T1. This mass shift could arise from either methylation or oxidation (e.g., Pro oxidation to a ketone). As this peak was not noted in C∼SP-B or H∼SP-B, but only in F∼SP-B, the results

suggest that oxidation of other residues, possibly a Pro to a ketonic Pro, occurred during Fenton oxidation. However, this possibility was not confirmed by tandem MS. Other small peaks, particularly in F∼SP-B, showed similar increases in mass, presumably due to oxidation.

Figure 6C (*m*/*z* 3065−3125) shows a peak at 3078.6 *m*/*z*, corresponding to T5 (G25−R52). A larger peak is observed at 3094.6 corresponding to an increment of 16 mass units. Thus, as with the previous spectra, partial oxidation of C∼SP-B is indicated, likely at Met29. With H∼SP-B and to a greater extent F∼SP-B, peak 3078.6 is barely detectable, while 3094.6 is elevated, reflecting the oxidation of Met residues in these peptides during exposure of BLES to ROS or during analysis.

Taken together, these mass spectra of SP-B tryptic fragments show oxidation-related mass increases indicative of the oxidative changes in Trp9, as inferred from the fluorescence data, and also provide evidence consistent with the oxidation of Met29 and Met65. Additional oxidation could possibly occur at Pro2, Pro4, and/or Pro6 to a minor extent during Fenton exposure. This could not be confirmed by MS/MS experiments due to the low intensities of these peaks.

Effect of Surfactant Phospholipid on SP-B Oxidation. The current and previous studies by our group have shown that, under the conditions employed, the Fenton reaction imparts a more serious impact on BLES biophysical function and BLES SP-B Trp fluorescence than exposure to hypochlorous acid. Earlier investigations on soluble and on membrane-associated proteins have demonstrated that hypochlorous acid can introduce structural alterations and modify Trp flurorescence. These considerations suggested the possibility that, as previously observed with other systems (*48*, *49*), the Trp residue in SP-B was being protected from the effects of hypochlorous acid through its interaction with surfactant lipids.

The manner by which the local environment of SP-B in BLES could affect ROS interactions with this low molecular weight hydrophobic protein was examined through reconstitution studies. Western blotting revealed (Figure 7A) that exposing isolated C∼SP-B to hypochlorous acid resulted in a marked decrease in anti-SP-B recognition relative to SP-B reconstituted with DPPC:POPG (7:3). Western blots showed that SP-B incubated in saline:1.5 mM $CaCl_2$, with and without Fe:EDTA, exhibited similar immunoreactivity whether the incubation was conducted in the presence or absence of PL. Slightly lower reactivity was evident in PL-containing samples exposed to Fenton reagents. When the PL was not present, SP-B reactivity was further decreased. These studies suggest that surfactant PL protects SP-B from oxidative degradation, at least to some extent.

DISCUSSION

Oxygen radicals are generated in the lung, as in all organs, as "escape" products from mitochondrial oxidative phosphorylation (see refs *12*, *14*, *15*, *21* for review). Pulmonary cells experience higher oxygen levels than cells in other organs, and these levels are increased during O_2 therapy. In addition, ROS are generated in the lung in vivo by intracellular and extracellular enzymes such as xanthine oxidase, which produces superoxide and hydrogen peroxide, and myeloperoxidase, which produces hypochlorous acid. Although the exact levels are unknown, detection of elevated lipid and other oxidation products in bronchoalveolar lavage demonstrates that ROS levels increase dramatically during ALI and ARDS (*12*, *14*, *15*). Elevated levels of ROS, such as HOCl, also arise through recruitment of activated neutrophils and other phagocytes. In the presence of extracellular transition metals such as iron, the nonenzymatic Fenton reaction generates hydroxyl radicals from hydrogen peroxide, which has been detected in normal bronchoalveolar lavage fluid and is greatly elevated with ALI and ARDS (*12*). Because the exact concentrations of neither ROS nor counteracting antioxidants in alveolar hypophase have been determined, we have applied oxidizing conditions established previously in order to facilitate comparison with former studies (*12*, *17*, *20*, *21*, *23*).

The present studies investigated the effects of hypochlorous acid and Fenton reaction products on SP-B structure and function. Exposing BLES, a clinical surfactant, to ROS resulted in time-dependent alterations in SP-B structure, as monitored by Coomassie Blue or silver staining and by Western blotting (Figure 1, Figure 2A,B) (*31*), using a specific antibody raised against porcine SP-B (*39*, *50*). Exposure to ROS led to depressed surface activity as demonstrated by studies where SP-B isolated from control (C∼SP-B), HOCl-treated (H∼SP-B), or Fenton-treated (F∼SP-B) BLES was formulated as DPPC:POPG:SP-B (70:30:1) and the mixtures were examined with the CBT. Adsorption of suspensions containing either H∼SP-B or F∼SP-B was retarded relative to control. H∼SP-B-containing surfactant was capable of reducing γ to near zero during the initial dynamic compression, but γ_{min} increased significantly during surface area cycling. Reconstituted surfactants containing F∼SP-B proved incapable of attaining low γs even during the initial compression. The failure to achieve low γ_{min}s during expiration would limit gaseous exchange, promote alveolar collapse, and favor lung edema (see refs *1*, *2*, *5* for review). Surfactants containing H∼SP-B or F∼SP-B also showed higher γ_{max} values during film expansion. Since surfactant adsorption from the bulk phase is far too slow to account for formation of a surface film near the equilibrium surface tension of ∼23 mN/m during surface area cycling, it is generally considered that γ_{max} is maintained near equilibrium by respreading of PL from multilayers associated with the surface monolayer (*1*, *3*, *4*, *34*, *35*). Increasing γ_{max} would increase the force required to inflate the lung and thus lead to a greater work of breathing. Increasing γ_{max} also tends to result in a higher γ_{min}.

Under the conditions used here, Fenton reactants generated a more deleterious effect on biophysical activity than HOCl. These observations implicate SP-B oxidation by either regimen in the deleterious effects of ROS on BLES biophysical activities and are in overall agreement with previous studies demonstrating protein oxidation to be a contributing factor in surfactant inhibition (*18*, *20*, *22*, *51*, *52*) during oxidative stress and that SP-B represents an oxidative target (*19*, *23*). They also show that HOCl and Fenton reagents have distinct effects on SP-B biophysical activity.

Trp acts as a key amino acid residue in a large number of proteins, and Trp modifications have been implicated in loss of activity of a number of proteins, including α and β crystallins (*44*, *53*); nitric oxide synthetase (*54*); peroxidases

(*55*); Cu, Zn superoxide dismutases (*47*); α-1-microglobin (*56*); myoglobin (*57*); cytochrome *c* peroxidase (*58*); ribonucleotide reductase (*59*); and surfactant protein-A (*60*) (see refs *61*−*65* for review). The present studies using previously established protocols (*44*, *45*) indicated that while HOCl moderately affected Trp intrinsic fluorescence, F reactants virtually abolished Trp fluorescence and induced formation of Kyn and NFKyn (Figure 4).

Examination of C∼SP-B, H∼SP-B, and F∼SP-B by ESI-MS provided evidence for partial oxidation of the control protein, possibly during incubation at 37 °C, isolation, and analysis as has been commonly observed with other proteins (*46*, *66*). H∼SP-B showed enhanced oxidation, consistent with reduced biophysical activity, while F∼SP-B was altered to such an extent that the ESI-MS spectra could hardly be obtained. However, although the ESI-MS spectra suggested prominent structural modification, examination of trypsin-derived fragments T1, T5, T6, T7 indicated that major amino acid alterations appeared primarily limited to Trp and Met. MALDI spectra of T1 revealed increases of 4, 16, 32, and 48 Da over the anticipated peak, suggesting the formation of Kyn from Trp (+4) and the addition of one to three oxygens to the N-terminal region of SP-B. While detected with C∼SP-B T1, the oxygenated peaks were elevated with H∼SP-B and greatly increased with F∼SP-B. This suggests that the major oxidative alterations to the N-terminal region can likely be attributed to modification of Trp9, resulting in formation of at least some OHTrp and perhaps some DiOHTrp and Tri-OHTrp. Because it is plausible that some of the recorded mass increments could arise from oxidation of Phe1 or Tyr7 (or a combination of Trp, Phe, and Tyr oxidation), the peptide fragments were subjected to MS/MS analysis. This generated amino acid fragments corresponding to Trp oxidation without any major evidence for oxidation of the other two aromatic amino acids, consistent with the observation that similar overall fluorescence effects were observed when SP-Bs were excited at E_{ex} 295 which would preclude significant effects on Tyr. MS/MS also confirmed that, with Fenton exposure, the +32 Da peak at 1653.8 represents the formation of NFKyn in accordance with the E_{ex} fluorescence spectral data (Figure 4). The elevation in the +4 Da peak in T1 from F∼BLES represents a signature alteration for increased Kyn levels in F∼BLES, as suggested by the fluorescence data and confirmed by tandem MS (data not shown). These analyses provide strong support for our conclusion that C∼SP-B contains hydroxylated Trp residues and these are marginally increased during the 24 h exposure to HOCl. Fenton reaction further modifies Trp9 to produce NFKyn and Kyn.

The T1 fragment from F∼SP-B also exhibited a small increase in +14 Da (Figure 6B). This latter alteration could reflect either oxidation to Pro2, Pro4, Pro6, or else methylation, possibly at the N-terminus of SP-B. Since methylation did not occur to a significant extent during extraction, isolation, or incubation of SP-B with C∼BLES or H∼BLES, it appears possible that the most likely explanation of the +14 increase would be N-terminal methylation and/or Pro ketonization although this could not be proven by tandem MS. As elaborated below, exposing BLES to ROS also led to oxidation of Met29 and 65, particularly Met65. In this case, elevated oxidation was observed with both HOCl and the Fenton reaction.

These observations and interpretations are in good overall agreement with previous studies on protein oxidation. For example, Zhang et al. (*45*, *47*) report induction of bicarbonate-mediated peroxidase activity of human superoxide dismutase is accompanied by the oxidation of Trp to OHTrp, which then undergoes oxidative cleavage to NFKyn and Kyn. Likewise, intrinsic fluorescence spectroscopy and tandem mass spectrometry have been used to show that UV irradiation of α-A lens crystallin results in conversion of Trp to NFKyn (*44*, *46*). These alterations were accompanied by Met oxidation, the racemization of an Asp residue, and alteration of secondary structure, thereby explaining the reduced chaperon-like activity of the irradiated protein.

Exposure of BLES to ROS resulted in the loss of SP-B-dependent surface activity. Reconstituted surfactants containing DPPC:POPG: H∼SP-B were able to achieve low γs during the initial quasi-static and dynamic compressions, but surface activity declined thereafter. DPPC:POPG:F∼SP-B surfactants were not capable of attaining low γs, even during the initial compressions. These results concur with previous observations on the effects of ROS, where the major effect of HOCl was to reduce respreadability of BLES PL, while the major effect of the Fenton reaction was to disrupt the ability of adsorbed films to achieve low γs during compression (*23*, *31*). It is important to note that Fenton reaction also affects PL respreading negatively, but this deficiency was more difficult to detect due to the massive effects on γ reduction. Taken together, the results are consistent with the interpretation that Met oxidation, which occurs to a considerable extent with both HOCl and Fenton, affects the ability of SP-B to promote respreading of BLES PL. Oxidation of SP-B by the Fenton reaction further abrogates SP-B function, such that DPPC:POPG:F∼SP-B films cannot achieve γs near zero during the initial lateral compression.

It is plausible that this latter biophysical property related to Fenton exposure is dependent on the greatly increased Trp modification, especially the selective formation of Kyn observed with Fenton relative to HOCl. A specific role for Trp9 in SP-B biophysical activity has been indicated by insightful studies on SP-B peptides by Ryan et al. (*67*). These investigators examined the ability of peptides based on one or more SP-B helical regions to interact with DPPC:POPG (7:3) vesicles. Helices 1 and 2 are thought located in the N-terminus (∼7−22 and 23−42) while helices 3−5 are localized to the C-terminus (∼43−79) of SP-B (*26*, *67*, *68*). These studies examined the ability of intact SP-B and SP-B peptides to promote aggregation (i.e., clumping), membrane lysis (leakage of water-soluble fluorescent probes encapsulated within the vesicles), and lipid mixing (diffusion of fluorescent membrane probes present in the outer PL leaflet onto the outer leaflet of another vesicle. Note that this is hemi-fusion. With true fusion, both leaflets would interact and the combined contents would be retained within the newly formed larger vesicle). They found that helix 1 (residues 7−22) induced membrane lysis while helix 2 (residues 23−42) promoted membrane aggregation (vesicle cross-linking). Using CBT assays, it was observed that the specific ability to achieve low γs during compression−expansion cycling required the initial nonhelical N-terminal region, helix 1 and helix 2 (SP-B 1−37). The C-terminal half of SP-B (SP-B 43−79), which contains helices 3, 4, and 5, possessed significantly lower lytic, fusogenic, and

surface tension-reducing capacities. In keeping with the observations reported here, replacing Trp9 of SP-B 1−37 with Ala resulted in elevated γ_{min} ($\geq$15 vs $<$2 mN/m). Similar observations were reported more recently by Serrano et al. (*68*). These observations would suggest that Trp9 modification can interfere with γ reduction during compression in the absence of Met oxidation. However, it must be stressed that these groups also found that exchanging Pro2, Pro4, and Pro6 with Ala increased γ_{min} to $\leq$10 mN/m. Although the Fenton effects on biophysical activity noted here could possibly also arise from alterations in Pro, the observed increase in the +14 Da peak at 1635.8 of T1 is small relative to the combined alterations in Trp9, suggesting that modification of the latter amino acid produced the major effect. Ryan et al. (*67*) also reported that converting Pro23 to Ala increased γ_{min}. It is considered that Pro23 is important in orienting helix 1 and helix 2 of SP-B. Unfortunately, our MALDI-MS experiments did not provide information on the tryptic peptide containing this residue because the fragment was too small to be detected under our experimental settings. We note that there is no evidence for oxidation of Pro67 in T7 (Figure 6A). Nevertheless, ambiguities induced by the potential partial oxidation of Pro2, Pro4, and Pro6, and the lack of information on Pro23, preclude an absolute conclusion. Thus, although Trp9 is clearly critical for γ reduction with SP-B 1−37, our results implicating Trp modification as being specifically responsible for the loss of the ability to lower γ to low values clearly require confirmatory evidence. This is particularly true because while Fenton reaction and HOCl led to similar oxidation of Met29 (60−70%), Fenton reaction oxidized Met65 to a greater extent (~90% versus 60%). Thus it must be concluded that increased oxidation of either Trp9 or Met65 or both could contribute to the greater effects of Fenton oxidation.

In addition to the above considerations, an unanticipated finding was that ~half of Met29 was oxidized in the control isolated SP-B. Examination of nonincubated BLES revealed similar levels of oxidized Met29. Whether this oxidation was present in the alveolus in vivo or arose during surfactant isolation, during BLES preparation and storage, or during analysis is not known. Furthermore, the effect of Met29 oxidation on BLES activity in vivo and in vitro has not been determined, although it is clear that BLES has considerable physiological function in vivo (*2*, *69*).

The present studies show that Met29 and Met65 are differentially susceptible to oxidation under control conditions and when treated with HOCl or Fenton reagents. This susceptibility presumably relates to the environment around these residues. Whether this local effect is dependent on the nature of adjacent amino acids, results from the lipid environment, or both remains unknown. Nevertheless, it is clear that SP-B oxidation due to either HOCl or Fenton is mitigated by lipids. These results contrast with previous studies by Mark and Ingenito (*22*), who observed little difference in SP-A immunoreactivity when this hydrophilic surfactant apoprotein was exposed to oxidative conditions in the presence or absence of surfactant lipids.

At present, the manner in which the observed amino acid alterations negatively influence SP-B surfactant function is unknown. SP-B is a membrane surface protein which appears to interact with PL through its amphipathic helices (*3*, *8*, *9*, *26*, *27*, *28*). Replacement of the Arg and Lys residues in these helices with neutral amino acids greatly diminished their effects on surface tension reduction (*67*, *68*). These results suggest that the charged regions of these amphipathic helices interact with PL headgroups, particularly anionic PG. The present results further imply that increasing the polarity of the hydrophobic amino acids, Trp9, Met29, and Met65, through oxidation modifies SP-B helices, thereby interfering with membrane lysis and hemi-fusion. This would affect PL adsorption and film compressibility. When considered together with studies employing synthetic peptides containing one or more of these helices, it appears likely that oxidation of Trp9 likely represents the major inactivating event (*26*, *67*, *68*). However, as indicated earlier, the possibility that synergistic inhibitory effects arise from oxidation of two or more of these residues must be considered.

In summary, ROS treatment of BLES, a clinical surfactant, results in delayed adsorption and an impairment of the ability to attain low γs during film compression. This effect is accompanied by alterations in SP-B, as observed by Coomassie Blue and silver staining, by Western blotting, and by ESI-MS analysis. Fluorescence measurements found alterations in Trp9 with the Fenton reaction. Tryptic digestions revealed modification of Met65, Met29, and Trp9. Met29 was oxidized to a considerable extent (~50%) in control BLES. This oxidation was increased by HOCl and with Fenton reagents. Met65 was also oxidized, even in control BLES. This was increased with HOCl. After Fenton treatment, Met65 was almost completely oxidized. Control BLES contains small amounts of OHTrp and DiOHTrp. HOCl increased Trp9 oxidation. Fenton reaction increased the levels of these oxidative products and also resulted in formation of NFKyn and Kyn. Unreacted BLES also showed potential evidence for oxidized prolines in the N-terminal region of the protein, but this was very small. Thus, ROS inactivation of SP-B biophysical activity appears to involve modification of a maximum of three amino acids: Trp9, Met29, and Met65. The contribution of each of these residues to SP-B inactivation will require further study.

ACKNOWLEDGMENT

The authors gratefully acknowledge BLES Biochemicals, Inc., London, ON, for the contribution of surfactant for this research. Monoclonal anti-SP-B was received from Dr. Yoshiro Suzuki, Kyoto University, Sakyo-Kyoto, Japan. The assistance and advice of Ms. Anne Brickenden is gratefully acknowledged. We thank Dr. Stan Dunn (U. of Western Ontario) and Dr. Matthias Salathe (U. of Miami) for the use of their fluorometric equipment and Ms. Jessica Jia for technical advice with these instruments. The authors thank Dr. Julian Whitelegge (UCLA) for useful discussion.

REFERENCES

1. Possmayer, F. (2004) Physicochemical aspects of pulmonary surfactant. In *Fetal and Neonatal Physiology* (Polin, R. A., Fox, W. W., and Abman, S. H., Eds.) Vol. 2, pp 1014−1034, W. B. Saunders Company, Philadelphia.
2. Lewis, J. F., and Veldhuizen, R. (2003) The role of exogenous surfactant in the treatment of acute lung injury, *Annu. Rev. Physiol. 65*, 613−642.
3. Whitsett, J. A., and Weaver, T. E. (2002) Hydrophobic surfactant proteins in lung function and disease, *N. Engl. J. Med. 347*, 2141−2148.

4. Cole, F. S. (2003) Surfactant protein B: unambiguously necessary for adult pulmonary function, *Am. J. Physiol. 285*, L540−542.
5. Bachofen, H., and Schurch, S. (2001) Alveolar surface forces and lung architecture, *Comp. Biochem. Physiol., Part A: Mol. Integr. Physiol. 129*, 183−193.
6. McCormack, F. X., and Whitsett, J. A. (2002) The pulmonary collectins, SP-A and SP-D, orchestrate innate immunity in the lung, *J. Clin. Invest. 109*, 707−712.
7. Veldhuizen, R., and Possmayer, F. (2004) Phospholipid metabolism in lung surfactant, *Subcell. Biochem.: Membr. Dyn. Domains 37*, 359−388.
8. Nogee, L. M. (2004) Alterations in SP-B and SP-C expression in neonatal lung disease, *Annu. Rev. Physiol. 66*, 601−623.
9. Weaver, T. E., and Conkright, J. J. (2001) Function of surfactant proteins B and C, *Annu. Rev. Physiol. 63*, 555−578.
10. Lewis, J. F., and Brackenbury, A. (2003) Role of exogenous surfactant in acute lung injury, *Crit. Care Med. 31*, S324−328.
11. McCabe, A. J., Wilcox, D. T., Holm, B. A., and Glick, P. L. (2000) Surfactant−a review for pediatric surgeons, *J. Pediatr. Surg. 35*, 1687−1700.
12. Rodriguez-Capote, K., Faulkner, J. R., Nag, K., and Possmayer, F. (2005) Alteration of alveolar surfactant function by reactive oxygen species. In *Lung Surfactant Function and Disorder* (Nag, K., Ed.) Vol. 201, pp 425−448, Taylor & Francis, Boca Raton.
13. Spragg, R. G., and Lewis, J. F. (2001) Pathology of the surfactant system of the mature lung: second San Diego conference, *Am. J. Respir. Crit. Care Med. 163*, 280−282.
14. Hickman-Davis, J. M., Fang, F. C., Nathan, C., Shepherd, V. L., Voelker, D. R., and Wright, J. R. (2001) Lung surfactant and reactive oxygen-nitrogen species: antimicrobial activity and host-pathogen interactions, *Am. J. Physiol. 281*, L517−523.
15. Lang, J. D., McArdle, P. J., O'Reilly, P. J., and Matalon, S. (2002) Oxidant-antioxidant balance in acute lung injury, *Chest 122*, 314S−320S.
16. Devendra, G., and Spragg, R. G. (2002) Lung surfactant in subacute pulmonary disease, *Respir. Res. 3*, 19−33.
17. Andersson, S., Kheiter, A., and Merritt, T. A. (1999) Oxidative inactivation of surfactants, *Lung 177*, 179−189.
18. Bridges, J. P., Davis, H. W., Damodarasamy, M., Kuroki, Y., Howles, G., Hui, D. Y., and McCormack, F. X. (2000) Pulmonary surfactant proteins A and D are potent endogenous inhibitors of lipid peroxidation and oxidative cellular injury, *J. Biol. Chem. 275*, 38848−38855.
19. Gilliard, N., Heldt, G. P., Loredo, J., Gasser, H., Redl, H., Merritt, T. A., and Spragg, R. G. (1994) Exposure of the hydrophobic components of porcine lung surfactant to oxidant stress alters surface tension properties, *J. Clin. Invest. 93*, 2608−2615.
20. Haddad, I. Y., Zhu, S., Ischiropoulos, H., and Matalon, S. (1996) Nitration of surfactant protein A results in decreased ability to aggregate lipids, *Am. J. Physiol. 270*, L281−288.
21. Ingbar, D. H., Bair, R., Jung, P., Heinecke, J., and Haddad, I. Y. (1999) Hyperoxic lung injury increases HOCl-modified lung proteins and NA,K-adenosine triphosphatase nitrotyrosine content, *Chest 116*, 100S.
22. Mark, L., and Ingenito, E. P. (1999) Surfactant function and composition after free radical exposure generated by transition metals, *Am. J. Physiol. 276*, L491−500.
23. Rodriguez-Capote, K., Manzanares, D., Haines, T., and Possmayer, F. (2006) Reactive oxygen species inactivation of surfactant involves structural and functional alterations to surfactant proteins SP-B and SP-C, *Biophys. J. 90*, 2808−2821.
24. Zhai, Y., and Saier, M. H., Jr. (2000) The amoebapore superfamily, *Biochim. Biophys. Acta 1469*, 87−99.
25. Wang, Y., Rao, K. M., and Demchuk, E. (2003) Topographical organization of the N-terminal segment of lung pulmonary surfactant protein B (SP-B(1−25)) in phospholipid bilayers, *Biochemistry 42*, 4015−4027.
26. Waring, A. J., Walther, F. J., Gordon, L. M., Hernandez-Juviel, J. M., Hong, T., Sherman, M. A., Alonso, C., Alig, T., Braun, A., Bacon, D., and Zasadzinski, J. A. (2005) The role of charged amphipathic helices in the structure and function of surfactant protein B, *J. Pept. Res. 66*, 364−374.
27. Zaltash, S., Palmblad, M., Curstedt, T., Johansson, J., and Persson, B. (2000) Pulmonary surfactant protein B: a structural model and a functional analogue, *Biochim. Biophys. Acta 1466*, 179−186.
28. Perez-Gil, J., and Keough, K. M. W. (1998) Interfacial properties of surfactant proteins, *Biochim. Biophys. Acta 1408*, 203−217.
29. Schurch, S., Green, F. H. Y., and Bachofen, H. (1998) Formation and structure of surface films: captive bubble surfactometry, *Biochim. Biophys. Acta 1408*, 180−202.
30. Rahman, I., and MacNee, W. (1999) Lung glutathione and oxidative stress: implications in cigarette smoke-induced airway disease, *Am. J. Physiol. 277*, L1067−1088.
31. Rodriguez-Capote, K., McCormack, F. X., and Possmayer, F. (2003) Pulmonary Surfactant Protein-A (SP-A) Restores the Surface Properties of Surfactant after Oxidation by a Mechanism That Requires the Cys6 Interchain Disulfide Bond and the Phospholipid Binding Domain, *J. Biol. Chem. 278*, 20461−20474.
32. Bligh, E. G., and Dyer, W. J. (1959) A rapid method of total lipid extraction and purification, *Can. J. Biochem. Physiol. 37*, 911−917.
33. Curstedt, T., Johansson, J., Barros-Soderling, J., Robertson, B., Nilsson, G., Westberg, M., and Jornvall, H. (1988) Low-molecular-mass surfactant protein type 1. The primary structure of a hydrophobic 8-kDa polypeptide with eight half-cystine residues, *Eur. J. Biochem. 172*, 521−525.
34. Qanbar, R., Cheng, S., Possmayer, F., and Schurch, S. (1996) Role of the palmitoylation of surfactant-associated protein C in surfactant film formation and stability, *Am. J. Physiol. 271*, L572−580.
35. Rodriguez-Capote, K., Nag, K., Schurch, S., and Possmayer, F. (2001) Surfactant protein interactions with neutral and acidic phospholipid films, *Am. J. Physiol. 281*, L231−242.
36. Lowry, O. H., Rosebrough, N. J., Farr, A. L., and Randall, R. J. (1951) Protein measurement with the Folin reagent, *J. Biol. Chem. 193*, 265−275.
37. Yu, S. H., Chung, W., and Possmayer, F. (1989) Structural relationship between the two small hydrophobic apoproteins in bovine pulmonary surfactant, *Biochim. Biophys. Acta 1005*, 93−96.
38. Yu, S. H., Chung, W., Olafson, R. W., Harding, P. G., and Possmayer, F. (1987) Characterization of the small hydrophobic proteins associated with pulmonary surfactant, *Biochim. Biophys. Acta 921*, 437−448.
39. Suzuki, Y., Kogishi, K., Fujita, Y., Kina, T., and Nishikawa, S. (1986) A monoclonal antibody to the 15,000 dalton protein associated with porcine pulmonary surfactant, *Exp. Lung Res. 11*, 61−73.
40. Schoel, W. M., Schurch, S., and Goerke, J. (1994) The captive bubble method for the evaluation of pulmonary surfactant: surface tension, area, and volume calculations, *Biochim. Biophys. Acta 1200*, 281−290.
41. Shevchenko, A., Wilm, M., Vorm, O., and Mann, M. (1996) Mass spectrometric sequencing of proteins silver-stained polyacrylamide gels, *Anal. Chem. 68*, 850−858.
42. Rouser, G., Fleischer, S., and Yamamoto, A. (1970) Two dimensional thin layer chromatographic separation of polar lipids and determination of phospholipids by phosphorous analysis of spots, *Lipids 5*, 494−496.
43. Dubinina, E. E. (2001) [The role of reactive oxygen species as signal molecules in tissue metabolism in oxidative stress], *Vopr. Med. Khim. 47*, 561−581.
44. Fujii, N., Uchida, H., and Saito, T. (2004) The damaging effect of UV-C irradiation on lens alpha-crystallin, *Mol. Vis. 10*, 814−820.
45. Zhang, H., Andrekopoulos, C., Joseph, J., Chandran, K., Karoui, H., Crow, J. P., and Kalyanaraman, B. (2003) Bicarbonate-dependent peroxidase activity of human Cu,Zn-superoxide dismutase induces covalent aggregation of protein: intermediacy of tryptophan-derived oxidation products, *J. Biol. Chem. 278*, 24078−24089.
46. Schey, K. L., and Finley, E. L. (2000) Identification of peptide oxidation by tandem mass spectrometry, *Acc. Chem. Res. 33*, 299−306.
47. Zhang, H., Joseph, J., Crow, J., and Kalyanaraman, B. (2004) Mass spectral evidence for carbonate-anion-radical-induced posttranslational modification of tryptophan to kynurenine in human Cu, Zn superoxide dismutase, *Free Radical Biol. Med. 37*, 2018−2026.
48. Knott, H. M., Baoutina, A., Davies, M. J., and Dean, R. T. (2002) Comparative time-courses of copper-ion-mediated protein and lipid oxidation in low-density lipoprotein, *Arch. Biochem. Biophys. 400*, 223−232.
49. Yan, L. J., Lodge, J. K., Traber, M. G., Matsugo, S., and Packer, L. (1997) Comparison between copper-mediated and hypochlorite-

mediated modifications of human low density lipoproteins evaluated by protein carbonyl formation, *J. Lipid Res. 38*, 992−1001.
50. Kramer, H. J., Schmidt, R., Gunther, A., Becker, G., Suzuki, Y., and Seeger, W. (1995) ELISA technique for quantification of surfactant protein B (SP-B) in bronchoalveolar lavage fluid, *Am. J. Respir. Crit. Care Med. 152*, 1540−1544.
51. Haddad, I. Y., Ischiropoulos, H., Holm, B. A., Beckman, J. S., Baker, J. R., and Matalon, S. (1993) Mechanisms of peroxynitrite-induced injury to pulmonary surfactants, *Am. J. Physiol. 265*, L555−564.
52. Marzan, Y., Mora, R., Butler, A., Butler, M., and Ingenito, E. P. (2002) Effects of simultaneous exposure of surfactant to serum proteins and free radicals, *Exp. Lung Res. 28*, 99−121.
53. Sergeev, Y. V., Soustov, L. V., Chelnokov, E. V., Bityurin, N. M., Backlund, P. S., Jr., Wingfield, P. T., Ostrovsky, M. A., and Hejtmancik, J. F. (2005) Increased Sensitivity of Amino-Arm Truncated {beta}A3-Crystallin to UV-Light-Induced Photoaggregation, *Invest. Ophthalmol. Vis. Sci. 46*, 3263−3273.
54. Wang, Z. Q., Wei, C. C., Santolini, J., Panda, K., Wang, Q., and Stuehr, D. J. (2005) A tryptophan that modulates tetrahydrobiopterin-dependent electron transfer in nitric oxide synthase regulates enzyme catalysis by additional mechanisms, *Biochemistry 44*, 4676−4690.
55. Pogni, R., Baratto, M. C., Giansanti, S., Teutloff, C., Verdin, J., Valderrama, B., Lendzian, F., Lubitz, W., Vazquez-Duhalt, R., and Basosi, R. (2005) Tryptophan-based radical in the catalytic mechanism of versatile peroxidase from Bjerkandera adusta, *Biochemistry 44*, 4267−4274.
56. Sala, A., Campagnoli, M., Perani, E., Romano, A., Labo, S., Monzani, E., Minchiotti, L., and Galliano, M. (2004) Human alpha-1-microglobulin is covalently bound to kynurenine-derived chromophores, *J. Biol. Chem. 279*, 51033−51041.
57. Gunther, M. R. (2004) Probing the free radicals formed in the metmyoglobin-hydrogen peroxide reaction, *Free Radical Biol. Med. 36*, 1345−1354.
58. Barrows, T. P., Bhaskar, B., and Poulos, T. L. (2004) Electrostatic control of the tryptophan radical in cytochrome c peroxidase, *Biochemistry 43*, 8826−8834.
59. Chang, M. C., Yee, C. S., Stubbe, J., and Nocera, D. G. (2004) Turning on ribonucleotide reductase by light-initiated amino acid radical generation, *Proc. Natl. Acad. Sci. U.S.A. 101*, 6882−6887.
60. Wang, G., Bates-Kenney, S. R., Tao, J. Q., Phelps, D. S., and Floros, J. (2004) Differences in biochemical properties and in biological function between human SP-A1 and SP-A2 variants, and the impact of ozone-induced oxidation, *Biochemistry 43*, 4227−4239.
61. Svistunenko, D. A. (2005) Reaction of haem containing proteins and enzymes with hydroperoxides: the radical view, *Biochim. Biophys. Acta 1707*, 127−155.
62. Westerlund, K., Berry, B. W., Privett, H. K., and Tommos, C. (2005) Exploring amino-acid radical chemistry: protein engineering and de novo design, *Biochim. Biophys. Acta 1707*, 103−116.
63. Proshlyakov, D. A. (2004) UV optical absorption by protein radicals in cytochrome c oxidase, *Biochim. Biophys. Acta 1655*, 282−289.
64. Hoganson, C. W., and Tommos, C. (2004) The function and characteristics of tyrosyl radical cofactors, *Biochim. Biophys. Acta 1655*, 116−122.
65. Fitzpatrick, P. F. (2003) Mechanism of aromatic amino acid hydroxylation, *Biochemistry 42*, 14083−14091.
66. Taylor, S. W., Fahy, E., Murray, J., Capaldi, R. A., and Ghosh, S. S. (2003) Oxidative post-translational modification of tryptophan residues in cardiac mitochondrial proteins, *J. Biol. Chem. 278*, 19587−19590.
67. Ryan, M. A., Qi, X., Serrano, A. G., Ikegami, M., Perez-Gil, J., Johansson, J., and Weaver, T. E. (2005) Mapping and analysis of the lytic and fusogenic domains of surfactant protein B, *Biochemistry 44*, 861−872.
68. Serrano, A. G., Ryan, M., Weaver, T. E., and Perez-Gil, J. (2006) Critical structure-function determinants within the N-terminal region of pulmonary surfactant protein SP-B, *Biophys. J. 90*, 238−249.
69. Enhorning, G., Shennan, A., Possmayer, F., Dunn, M., Chen, C. P., and Milligan, J. (1985) Prevention of neonatal respiratory distress syndrome by tracheal instillation of surfactant: a randomized clinical trial, *Pediatrics 76*, 145−153.

BI062304P